

Original Research

CD6 and CCR7 as Genetic Biomarkers in Evaluating Intracranial Aneurysm Rupture Risk

Dan-Dan Xu^{1,*}, Xiao-Qiang Liu¹, Zhi-Sheng Wu^{1,*}¹Department of Neurology, Quanzhou First Hospital Affiliated to Fujian Medical University, 362000 Quanzhou, Fujian, China*Correspondence: xddxxs1102@163.com (Dan-Dan Xu); wzs740128@sina.com (Zhi-Sheng Wu)

Academic Editor: Hahn Young Kim

Submitted: 6 July 2023 Revised: 2 August 2023 Accepted: 18 August 2023 Published: 11 March 2024

Abstract

Background: This study used bioinformatics combined with statistical methods to identify plasma biomarkers that can predict intracranial aneurysm (IA) rupture and provide a strong theoretical basis for the search for new IA rupture prevention methods. **Methods:** We downloaded gene expression profiles in the GSE36791 and GSE122897 datasets from the Gene Expression Omnibus (GEO) database. Data were normalized using the “sva” R package and differentially expressed genes (DEGs) were identified using the “limma” R package. Gene Ontology (GO) and Kyoto Encyclopedia of Genes and Genomes (KEGG) pathway enrichment analyses were used for DEG function analysis. Univariate logistic regression analysis, least absolute shrinkage and selection operator (LASSO) regression modeling, and the support vector machine recursive feature elimination (SVM-RFE) algorithm were used to identify key biomarker genes. Data from GSE122897 and GSE13353 were extracted to verify our findings. **Results:** Eight co-DEG mRNAs were identified in the GSE36791 and GSE122897 datasets. Genes associated with inflammatory responses were clustered in the co-DEG mRNAs in IAs. *CD6* and C-C chemokine receptor 7 (*CCR7*) were identified as key genes associated with IA. *CD6* and *CCR7* were upregulated in patients with IA and their expression levels were positively correlated. There were significant differences in the infiltration of immune cells between IAs and normal vascular wall tissues ($p < 0.05$). A predictive nomogram was designed using this two-gene signature. Binary transformation of *CD6* and *CCR7* was performed according to the cut-off value to construct the receiver-operating characteristic (ROC) curve and showed a strong predictive ability of the *CD6-CCR7* gene signature ($p < 0.01$; area under the curve (AUC): 0.90; 95% confidence interval (CI): 0.88–0.92). Furthermore, validation of this two-gene signature using the GSE122897 and GSE13353 datasets proved it to be valuable for clinical application. **Conclusions:** The identified two-gene signature (*CD6-CCR7*) for evaluating the risk of IA rupture demonstrated good clinical application value.

Keywords: intracranial aneurysm; biomarker; rupture; bioinformatics analysis; differentially expressed gene

1. Introduction

An intracranial aneurysm (IA) is a fusiform, balloon-like bulge in a weak area of a blood vessel in the brain. It is caused by abnormal local changes in the intracranial arterial blood vessel walls, which may be a result of local congenital defects of the blood vessel wall muscle layers or degeneration of the internal elastic layer of the blood vessel wall under the influence of acquired factors that are simultaneously affected by other factors, including hemodynamics [1]. IAs constitute the main cause of spontaneous subarachnoid hemorrhage, and their bleeding probability is second only to that of ischemic stroke and hypertensive cerebral hemorrhage [2]. When an IA ruptures without warning, approximately one-third of patients reportedly die before reaching the hospital. With the advancements in surgical techniques and microscopic instruments, the diagnosis and treatment of IAs have improved in recent years [3–5]. However, if the ruptured aneurysm hemorrhages again, the mortality rate is 60–80%. Approximately half of the surviving patients endure moderate-to-severe lifetime disability, which can cause a significant economic burden to their families and society [6]. Studying and analyzing the risk factors

related to IA rupture can therefore help us to appropriately treat unruptured aneurysms in a timely manner, with obvious benefit to the patient.

Various factors cause IA rupture, including size and location of the IA, and patient-related risk factors such as chronic hypertension and cigarette smoking [7,8]. With recent developments in molecular biology, genetics, and other disciplines, our understanding of the differences between the walls of IA blood vessels and those of normal blood vessels, and the role of IA-related genes in the formation and rupture of IAs and their mechanism of action, has improved through genome and differential gene expression analyses, providing a strong basis for the development of new IA prevention and treatment methods [9,10]. An increasing number of researchers aim to identify effective biomarkers to monitor IA formation and rupture by revealing its etiology and pathogenesis [11]. Inflammatory cytokines such as matrix metalloproteinases (MMPs), Monocyte Chemoattractant Protein-1 (MCP-1), Tumor Necrosis Factor- α (TNF- α), and Zona Occludens 1 (ZO-1), directly or indirectly grafting, promote the growth and rupture of IAs [12,13]. Pan *et al.*'s [14] study showed that the level



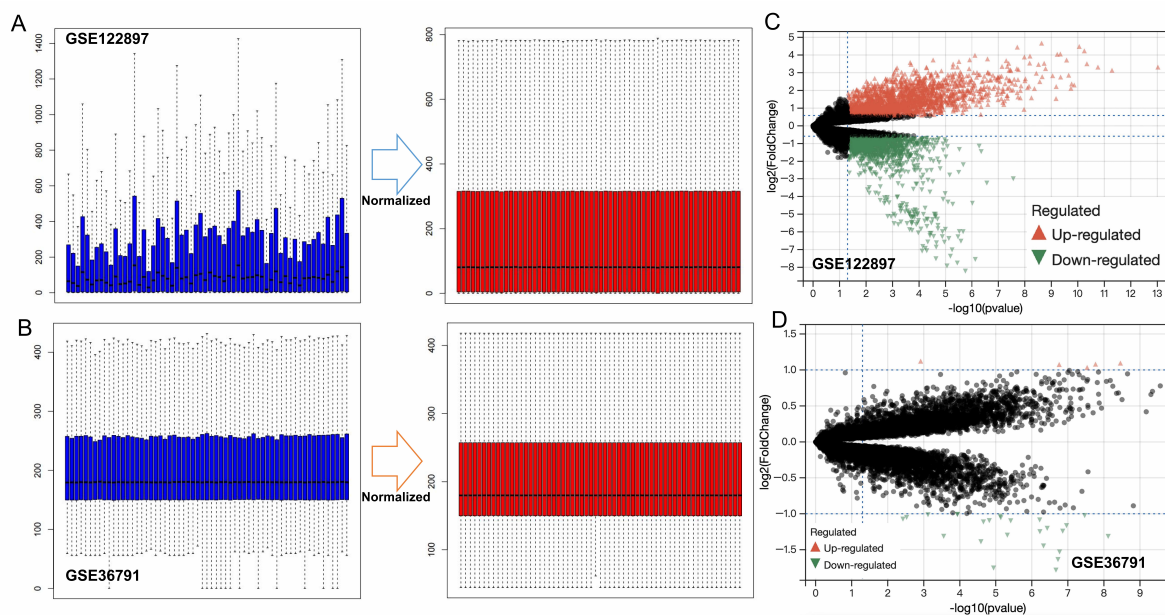


Fig. 1. Differentially expressed gene analysis. (A,B) Merged and normalize the chip data (GSE122897 and GSE36791) in the Gene Expression Omnibus (GEO) database. (C,D) Volcano plot of the differentially expressed genes (DEGs). Red and green dots represent genes that are significantly up- or down-regulated ($|\log_2FC| > 1$ and $p < 0.05$). FC, fold change.

of coagulin is an effective tool for predicting the mortality of aneurysms with subarachnoid hemorrhage. The aim of this study was to identify plasma biomarkers, using bioinformatics combined with statistical methods, that can predict IA rupture and provide a strong theoretical basis for the development of new IA prevention and treatment methods.

2. Methods

2.1 Differentially Expressed Gene Screening

The expression profiling (mRNA) datasets GSE36791 and GSE122897 were downloaded from the Gene Expression Omnibus (GEO) database (<https://www.ncbi.nlm.nih.gov/geo/>). The GSE36791 dataset (plasma samples) contained 43 patients with ruptured aneurysm (subarachnoid hemorrhage) and 18 control group patients (people with unruptured IA). The GSE122897 dataset (arterial tissue samples) contained 44 patients with ruptured aneurysm (subarachnoid hemorrhage) and 16 control group patients. The GSE36791 and GSE122897 datasets were normalized using the “sva” package (<http://www.bioconductor.org/>) respectively. Differentially expressed genes (DEGs) were identified using the “limma” R package (<http://www.bioconductor.org/>). Statistical significance was set at $|\log_2\text{Fold change} (\log_2FC)| > 1$ and $p < 0.05$. DEGs occurring in both datasets (co-DEGs) were identified using Venn analysis.

2.2 Functional Annotation of Gene Modules

Gene ontology (GO) enrichment analysis was used to annotate the cellular components (CCs), biological pro-

cesses (BPs), and molecular functions (MFs) of the DEGs. The biological pathways and functions of the DEGs were analyzed using the Kyoto Encyclopedia of Genes and Genomes (KEGG) database (<https://www.kegg.jp/>). Statistical significance was set at $p < 0.05$.

2.3 Statistical Analysis

The Student’s *t*-test was used for normally distributed variables. The Wilcoxon rank-sum test was used for non-normally distributed variables. The χ^2 test was used to compare categorical variables. Infiltrating immune cell scores and immune-related pathway activities were analyzed using single-sample gene set enrichment analysis (ss-GSEA). The support vector machine recursive feature elimination (SVM-RFE) “e1071” packages algorithm, random forest algorithm (“randomForest” package), and least absolute shrinkage and selection operator (LASSO) algorithm (“glmnet” package) were used to identify genes involved with IA rupture (<https://www.rdocumentation.org/>). The receiver-operating characteristic (ROC) curve was used to assess the reliability of the hub genes to predict an IA rupture. The area under the curve (AUC) was also measured, shown as the absolute value and 95% confidence interval (CI). All data analyses and graph generation were performed using SPSS version 25.0 (IBM Corp, Armonk, NY, USA), R version 4.1.1 (<https://www.r-project.org/>), and GraphPad Prism 8.0 (GraphPad Software, Inc., San Diego, CA, USA). Statistical significance was set at $p < 0.05$.

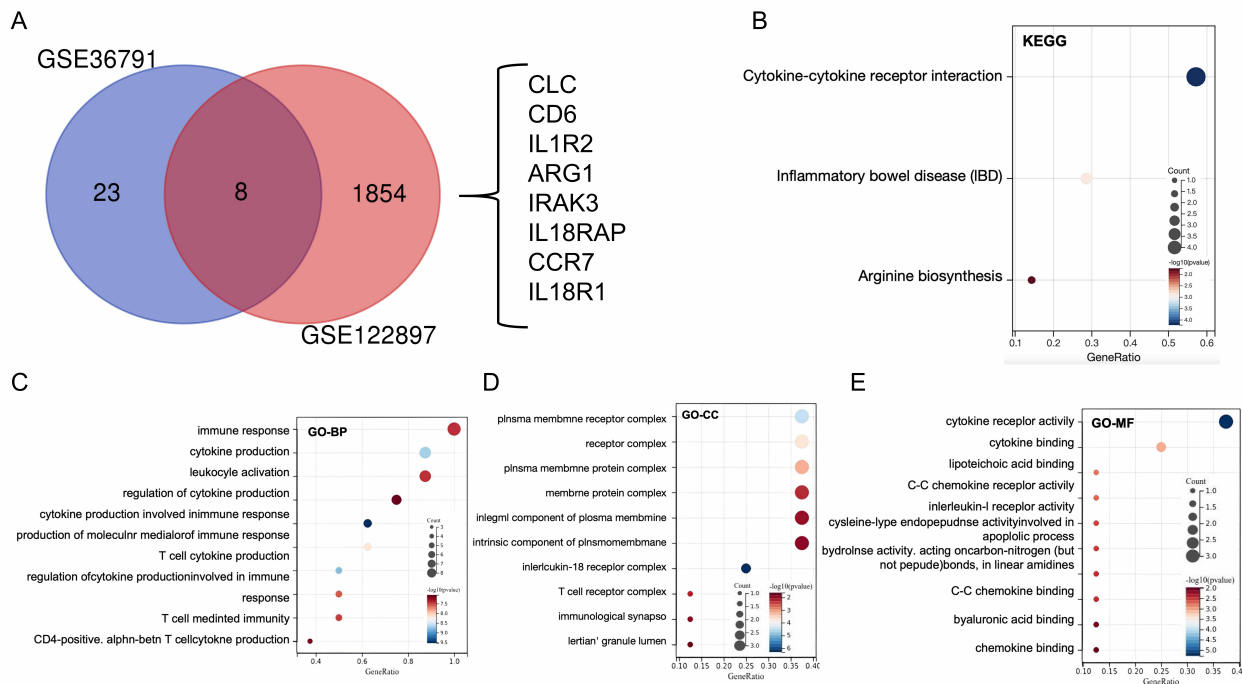


Fig. 2. DEG functional annotation. (A) Venn analysis between the DEGs from GSE36791 and GSE122897. Bubble charts showing the KEGG (B) and GO analysis results (including GO_BP (C), GO_MF (D) and GO_CC (E)) for eight co-DEG mRNAs. The size of the points represent the number of genes in the representative pathway. GO, gene ontology; BP, biological process; CC, cellular component; MF, molecular function; KEGG, Kyoto Encyclopedia of Genes and Genomes; mRNA, messenger RNA.

Table 1. Cut-off values of CD6 and CCR7.

Test result variable	Cut-off value	Area under curve	Standard error	95% CI	<i>p</i>
<i>CD6</i>	1.22	0.99	0.42	0.82–0.98	0.00
<i>CD6</i> > Cut-off values/ <i>CD6</i> High	/	0.85	0.56	0.74–0.96	0.00
<i>CCR7</i>	2.21	0.86	0.61	0.71–0.97	0.00
<i>CCR7</i> > Cut-off values/ <i>CCR7</i> High	/	0.84	0.67	0.51–0.84	0.00

CI, confidence interval.

3. Results

3.1 DEG Screening

Two microarray datasets (GSE36791 and GSE122897) were used in this study. The datasets were normalized and the DEGs were identified based on $p < 0.05$ and $|\log_{2}FC| > 1$ (Fig. 1A,B). Thirty-one DEG mRNAs were identified in the GSE36791 dataset and 1862 DEG mRNAs were identified in the GSE122897 dataset. The volcano plots show the DEG mRNAs in the arterial tissue (GSE122897; Fig. 1C) and plasma (GSE36791; Fig. 1D) samples between patients with IA and control individuals. Eight co-DEGs were identified using Venn analysis of the DEGs from GSE36791 and GSE122897 (Fig. 2A).

3.2 Functional Annotation of Gene Modules

The “Cluster Profiler” package used to perform the GO and KEGG pathway enrichment analyses to determine the function of eight co-DEG mRNAs. KEGG pathway analyses revealed that the eight co-DEGs were enriched for cytokine-cytokine receptor interaction, inflammatory bowel disease, and arginine biosynthesis pathways (Fig. 2B). The top three terms included immune response, cytokine production, and leukocyte activation in the biological process category. The enriched terms were related to plasma membrane receptor complex, receptor complex, and plasma membrane protein complex in the cellular component category. The enriched terms mainly included cytokine receptor activity, cytokine binding, and lipoteichoic acid binding in the molecular function category (Fig. 2C–E).

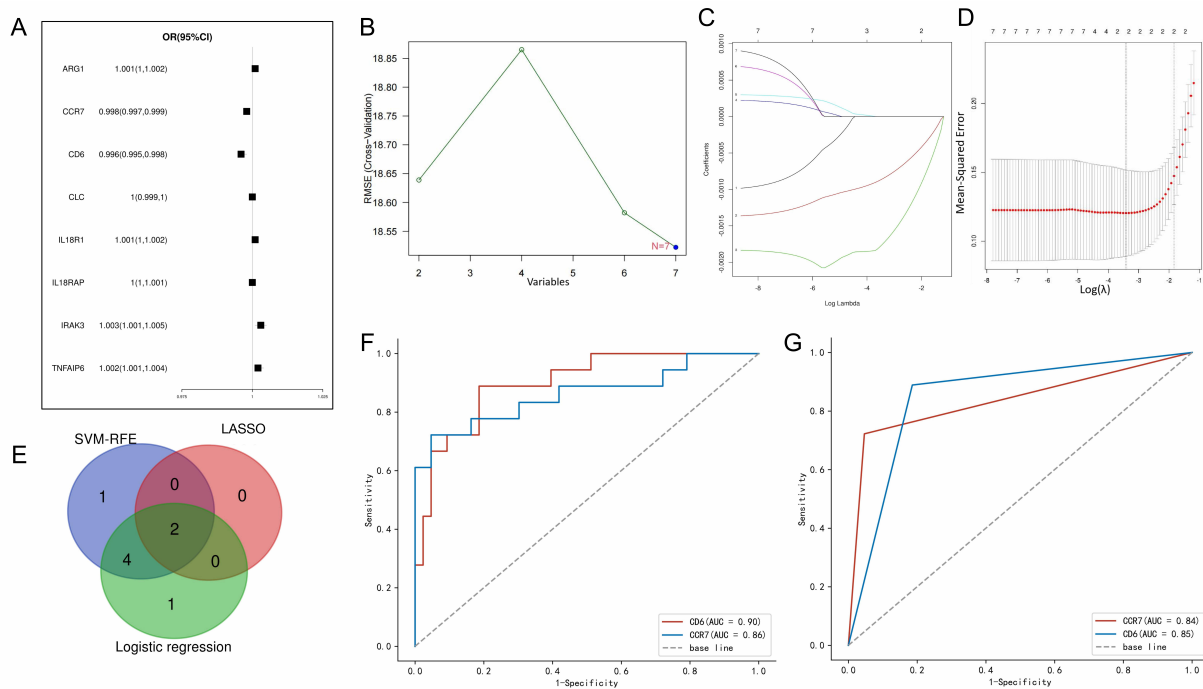


Fig. 3. Filter predictors of hub DEGs. (A) Binary logistic regression identification of key DEGs. The binary logistic regression algorithm was used to identify seven DEGs (*ARG1*, *CCR7*, *CD6*, *CLC*, *IL18RAP*, *IRAK3*, and *ILIR2*) as potential diagnostic markers for intracranial aneurysm rupture. (B) Biomarker selection using the support vector machine recursive feature elimination (SVM-RFE) algorithm. (C) Least absolute shrinkage and selection operator (LASSO) logistic regression identification of hub DEGs. (D) Optimal parameter (lambda) selection in the LASSO model used fivefold cross-validation via minimum criteria. (E) Venn diagram showing genes identified by all methods. (F,G) According to the cut-off value, binary transformation of *CD6* and *CCR7* was performed to construct the receiver-operating characteristic (ROC) curve. *CCR7*, C-C chemokine receptor 7; AUC, area under the curve.

3.3 Construction and Effectiveness Test of the Predictive Model

Univariate logistic regression analysis was performed on the eight co-DEG mRNAs in the GSE36791 dataset. The results suggested that *ARG1*, C-C chemokine receptor 7 (*CCR7*), *CD6*, *CLC*, *IL18RAP*, *IRAK3*, and *ILIR2* could influence IA rupture (Fig. 3A). These seven genes were also identified as possible diagnostic markers using the SVM-RFE algorithm (Fig. 3B). In addition, using the data from these seven genes in 61 patients, two potential predictors based on non-zero coefficients in the LASSO regression model were identified (Fig. 3C,D). ROC AUC analysis indicated that the expression levels of *CD6* and *CCR7* show potential diagnostic value and that these may be regarded as biomarkers for ruptured IAs (Fig. 3E). Binary transformation of *CD6* and *CCR7* was performed according to the cut-off value to construct the ROC curve (Fig. 3F,G, Table 1). Binary logistic regression analysis revealed that *CD6* and *CCR7* were independent predictive factors of IA rupture (Table 2).

Nomogram maps were constructed to predict the probability of IA rupture in patients with IA using *CD6* and *CCR7* (Fig. 4A). The nomogram was validated using a calibration curve. The calibration plots indicate that the nomo-

Table 2. *CD6* and *CCR7* binary logistic regression analysis in IA samples.

Variable	IA	Control	<i>p</i>	B	OR	95% CI	<i>p</i>
<i>CD6</i>			0.00	2.82	11.49	1.78–74.03	0.01
<i>CD6</i> High	16	8					
<i>CD6</i> Low	2	35					
<i>CCR7</i>			0.00	2.44	16.78	2.43–115.73	0.00
<i>CCR7</i> High	13	2					
<i>CCR7</i> Low	5	41					

CI, confidence interval; IA, intracranial Aneurysm; OR, odds ratio; B, Regression coefficient.

gram performed well in predicting the rupture probability in patients with IA (Fig. 4B,C). The AUC indicates that *CD6* and *CCR7* (in the nomogram model) more accurately predict the rupture probability in patients with IA. The ROC curve of the nomogram model was evaluated and the AUC was found to be 0.90 (Fig. 4D). These results suggest that the nomogram constructed using the two-gene signature has high accuracy in predicting the rupture probability in patients with IA. In addition, *CD6* and *CCR7* were upregulated in patients with IA and their expression levels were positively correlated (Fig. 4E,F).

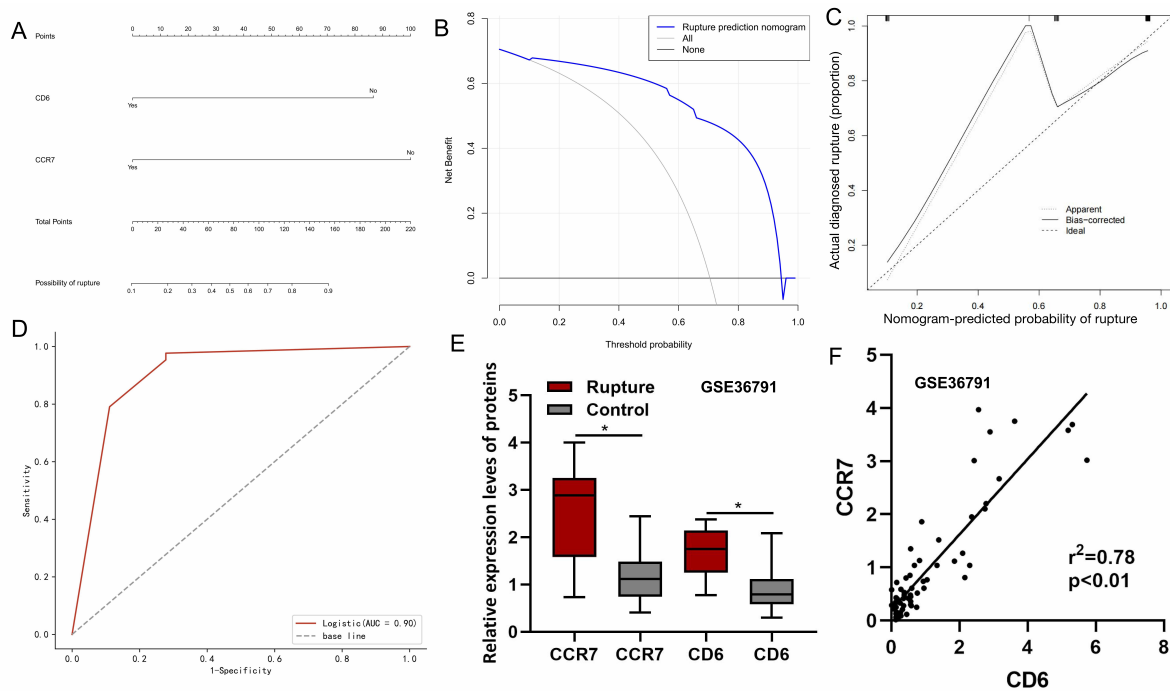


Fig. 4. Construction of the predictive model. (A) A ruptured intracranial aneurysm (IA) nomogram was constructed for *CD6* and *CCR7*. Each gene is given a score; the total score is calculated by adding each score and projecting this onto a lower total score scale. (B) Calibration curves of the ruptured IA nomogram prediction. The y-axis represents net benefit. The blue line represents the nomogram. The gray line represents all patients. The net benefit is calculated by subtracting the proportion of all false-positive patients from the proportion of true positives. (C) Calibration plot of predicted ruptured IAs, where actual probability is the actual outcome. Each dot mark at the top represents a patient. The x-axis represents the estimated ability to predict IA rupture derived from the nomogram and the y-axis represents the actual ability. (D) Receiver operating characteristic analysis of the ruptured IA nomogram. (E) *CD6* and *CCR7* mRNA expression in the ruptured IA and control groups in the GSE36791 dataset. * $p < 0.05$. (F) *CD6* and *CCR7* expression levels are positively correlated in the GSE36791 dataset.

These key genes were validated using the GSE122891 and GSE13353 datasets. *CD6* and *CCR7* were upregulated in patients with IA and their expression levels were significantly positively correlated (Fig. 5A1,A2,B1,B2). Hence, *CD6* and *CCR7* show potential diagnostic value ($p < 0.05$). The ROC curves for *CD6* and *CCR7* are shown in Fig. 5A3,B3.

3.4 Immune Cell Infiltration Analysis

We analyzed immune cell infiltration and immune cell function in the ruptured IA and control groups (Fig. 6A) Heat map showing differential immune cell infiltration and immune functions between the ruptured IA and control groups (Fig. 6B). Heat map showing correlations between immune cell infiltration and (Fig. 6C) immune functions. Immune cell infiltration analysis showed that $CD8^+$ T, mast, macrophage, Th1, Th2, T helper, Tfh, TIL, and Treg cells were up-regulated in IA patients compared with normal patients. Immune cell function analysis showed that cytolytic activity, antigen presenting cell (APC) co-inhibition, APC co-stimulation, inflammation-promotion, CCR, T cell co-inhibition, human leukocyte antigen (HLA), major his-

tocompatibility complex (MHC) class I, cell cycle checkpoint, para-inflammation, T cell co-stimulation, and Type II interferon (IFN) response functions were more active in IA patients compared with normal patients. Additionally, we performed correlation analysis between the up-regulated cells (Fig. 6B) and between the functions found to be more active in the IA group (Fig. 6C). Differential immune cell infiltration and immune functions between the ruptured IA and control groups show in Fig. 6D.

Furthermore, we performed correlation analysis between the differentially infiltrated immune cells identified above and *CCR7* and *CD6* respectively. *CCR7* was positively correlated with activated mast cells, neutrophils, M0 macrophages, and activated dendritic cells, but significantly negatively correlated with M2 macrophages M2, activated natural killer (NK) cells, resting dendritic cells, and M1 macrophages (Fig. 7A). *CD6* was positively correlated with neutrophils, plasma cells, activated mast cells, activated dendritic cells, and resting NK cells, but significantly negatively correlated with activated NK cells, M1 macrophages, resting dendritic cells, and M2 macrophages (Fig. 7B).

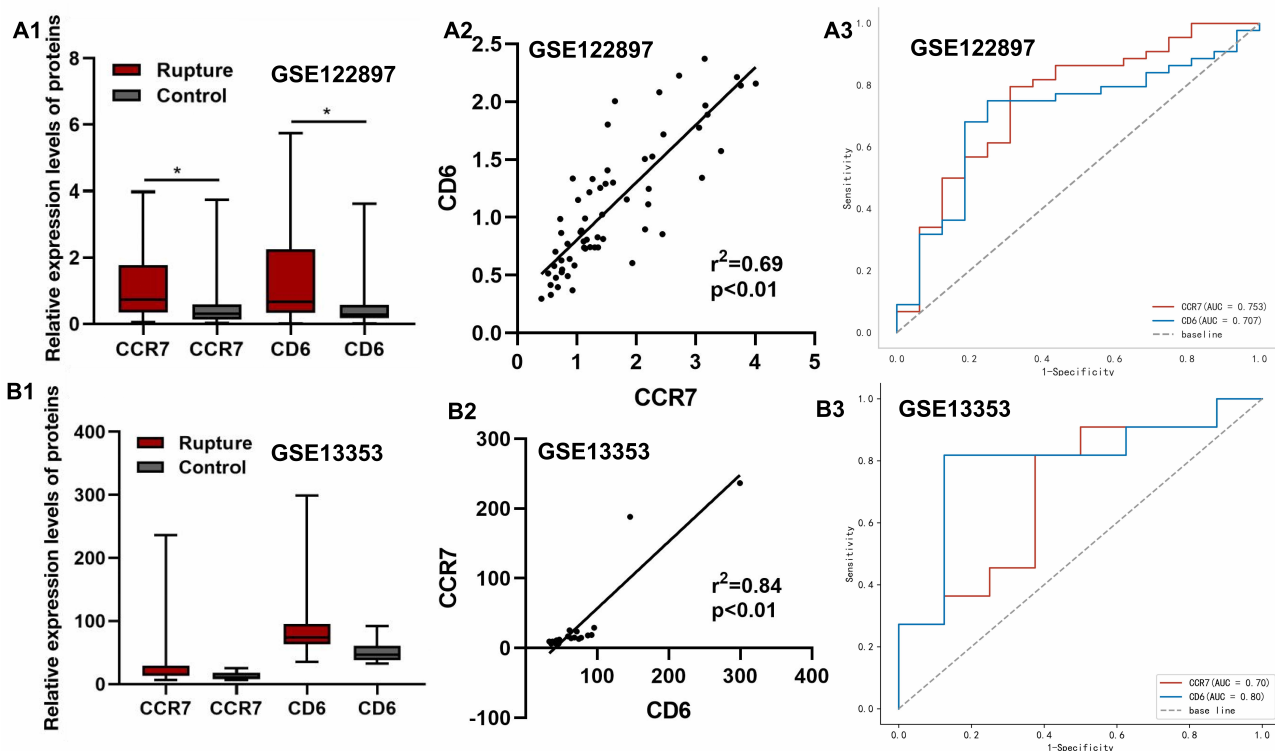


Fig. 5. Effectiveness test of the predictive model. (A1,B1) *CD6* and *CCR7* expression levels in the ruptured IA and control groups (GSE122897 and GSE13353 datasets), $*p < 0.05$. (A2,B2) *CD6* and *CCR7* expression are positively correlated in the GSE122897 and GSE13353 datasets. (A3,B3) Receiver operating characteristic curves indicate the predictive value of *CD6* and *CCR7* ruptured IA and control groups (GSE122897 and GSE13353 datasets).

4. Discussion

To identify differentially expressed mRNAs between the IA and control groups, high-throughput ChIP-sequencing data were extracted from the aorta tissue and plasma of patients. Based on the co-DEG mRNAs, nomogram maps were constructed to predict the rupture probability in patients with IA using bioinformatics and statistical analysis. The GSE122891 and GSE13353 datasets were used for validation. The transcriptional levels of *CD6* and *CCR7* were increased in patients with IA compared with those in control individuals, and the expression of *CD6* was significantly and positively correlated with that of *CCR7*. Furthermore, functional annotation of the co-DEG mRNAs, particularly those associated with inflammation-related signaling pathways, was performed.

In recent years, with the advances in IA research, it has been demonstrated that extracellular mechanisms of chronic inflammation and pathological remodeling of the arterial wall may be associated with the occurrence and development of IA [15]. Studies show that while inflammatory cells may infiltrate the normal arterial wall, large quantities of inflammatory cells are found in the arterial walls of IAs, which is related to the massive infiltration of immunoglobulins and macrophages during aneurysm formation [16,17]. Inflammatory cells can secrete cytokines,

which can cause abnormal secretion of pro-inflammatory factors by vascular endothelial and smooth muscle cells, thereby destroying the inner wall of the blood vessels. A variety of inflammatory cells and factor indicators, alone or in combination, have been identified as potential new immune and inflammatory response markers. These include the platelet to lymphocyte ratio, neutrophil to lymphocyte ratio and lymphocyte to mononuclear cell ratio, which have been shown to participate in the development and occurrence of cerebrovascular disease, and to be closely related to its prognosis [18–20]. Studies have shown that monocyte chemoattractant protein 1 (MCP1) upregulation in patients with aneurysm rupture is similar to that in patients with acute cerebral ischemia. This may be related to the inflammatory reactions in brain ischemia and tumor rupture caused by strong vasoconstriction in these patients [21,22]. MMPs are proteolytic enzymes that degrade the extracellular matrix, and increased MMP expression has been detected in aneurysms. The expression levels of MMP-9 and MMP-2 were significantly increased in patients with ruptured aneurysms compared with those with unruptured aneurysms [23].

Our study showed that the expression of *CCR7* and *CD6* were significantly upregulated in IA patients. Analysis of immune cell infiltration and function showed in-

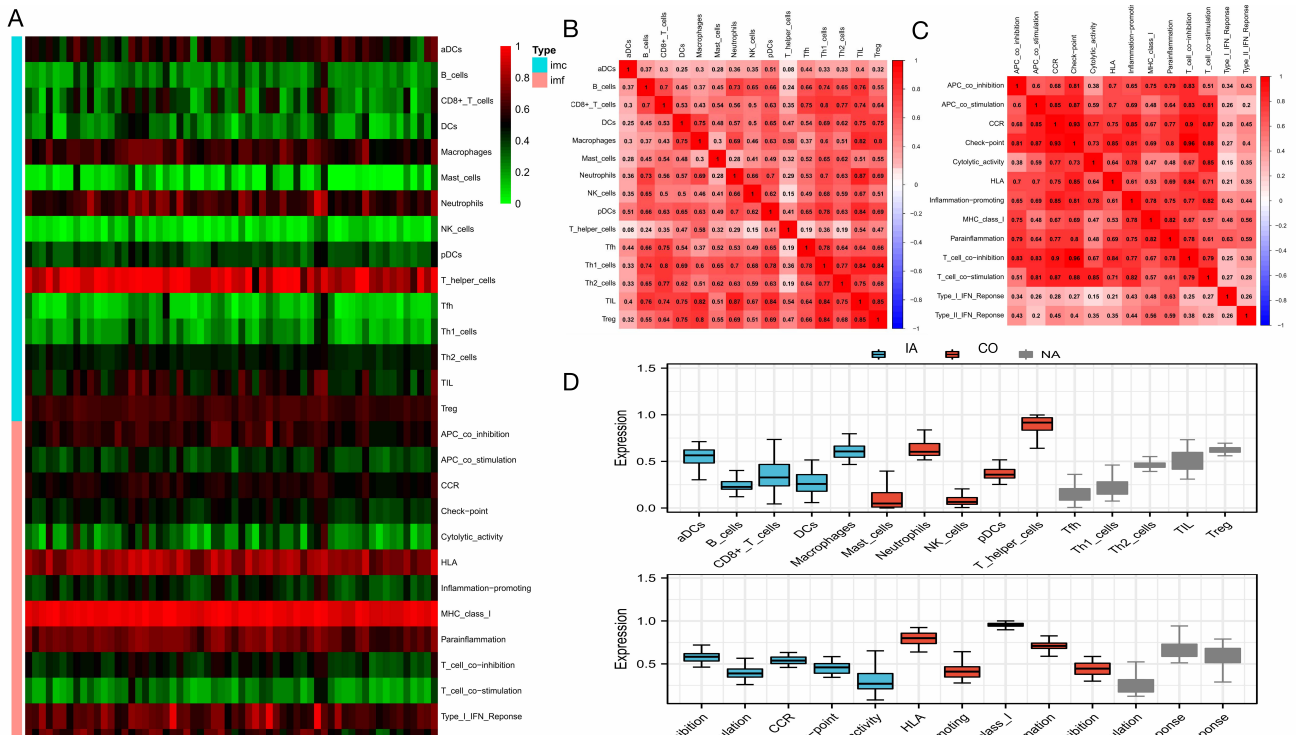


Fig. 6. Immune cell infiltration and immune function analysis. (A) Heat map showing differential immune cell infiltration and immune functions between the ruptured IA and control groups. (B,C) Heat map showing correlations between immune cell infiltration and immune functions. Numbers in the squares represent the strength of the correlation. The redder the color, the stronger the correlation. (D) Differential immune cell infiltration and immune functions between the ruptured IA and control groups. * $p < 0.05$; ** $p < 0.01$; *** $p < 0.001$, **** $p < 0.0001$. IA, Intracranial Aneurysm; CO, control.

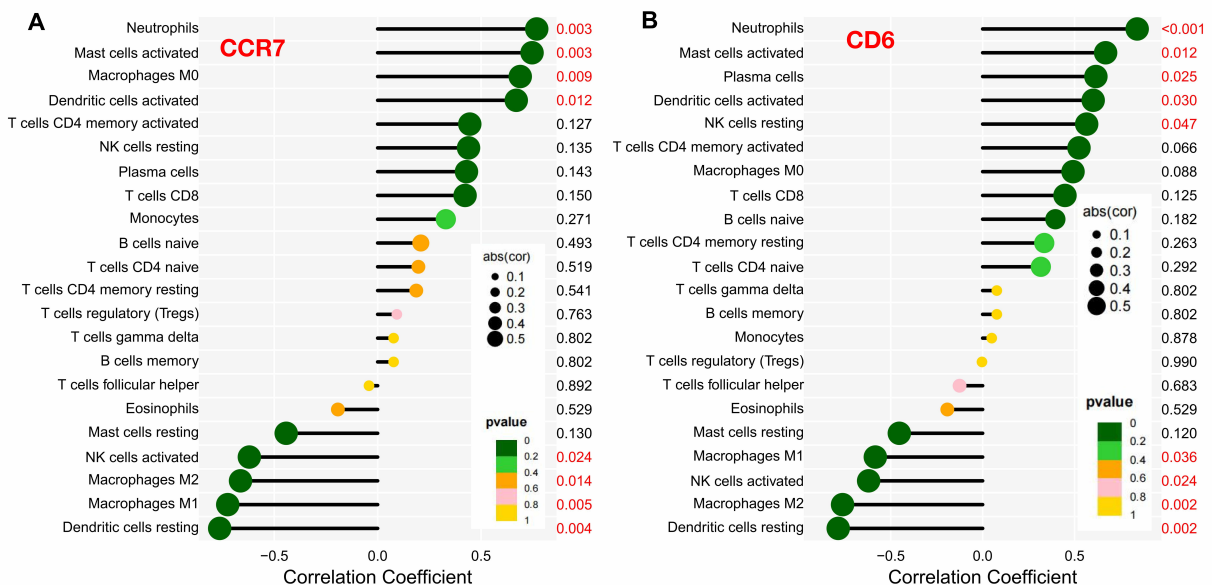


Fig. 7. Correlation analysis of infiltrating immune cells and functions. (A) Correlation between *CCR7* and infiltrating immune cells and functions in the ruptured IA group. (B) Correlation between *CD6* and infiltrating immune cells and functions in the ruptured IA group.

creased immune-inflammatory cell infiltration in IA, and *CCR7* and *CD6* expression was significantly positively correlated with immune-inflammatory cell functions. T cells

express *CD6*, a co-stimulatory membrane glycoprotein. *CD6* and its ligand can activate the leukocyte cell adhesion molecule (*ALCAM*), and they are involved in the activation

and trafficking of T cells [24]. This has been implicated in multiple autoimmune and inflammatory diseases, including multiple sclerosis, rheumatoid arthritis, and inflammatory bowel disease [25,26]. Chalmers *et al.* [27] demonstrated that the *CD6/ALCAM* pathway possibly promotes lupus nephritis through *CD6*, which is a strong biomarker of the disease. *CCR7* plays an important role in the immune response, mediating the delivery of antigens by dendritic cells to secondary lymphoid organs or tissues, and activating T lymphocytes to induce an immune response. *CCR7* is expressed in a variety of inflammatory and immune cells and participates in the regulation of inflammatory and immune responses [28,29]. Changes in *CCR7* expression have been reported to be closely associated with the progression of carotid atherosclerosis [30]. In atherosclerosis, *CCR7* promotes the adhesion and infiltration of macrophages to the vascular endothelium and the phagocytosis of oxidized low-density lipoproteins leading to the formation of foam cells, which accumulate lipids causing atherosclerotic plaque formation [31,32]. Llodrá *et al.* [33] proposed that *CCR7* signaling is critical for the outward migration of macrophages during the early stages of atherosclerosis resolution. Several factors can cause IA rupture. However, inflammation can directly cause wall degeneration and lead to IA enlargement, which is the key factor that ultimately increases rupture risk [34]. When the vascular wall is remodeled, it becomes decompensated by inflammation and cannot resist hemodynamic stress, resulting in aneurysm rupture [35].

Our study had some limitations. The results have not been confirmed by *in vitro* studies or other functional experiments. Although our results are based on the GEO database, we applied different statistical methods to validate the results and showcase our new findings. These results have certain implications for subsequent mechanism research.

5. Conclusions

Using bioinformatics and statistical analysis, we have shown that *CD6* and *CCR7* in inflammation-related signaling pathways are closely associated with IA rupture and may play an important role in its pathogenesis. Further studies are needed to investigate the potential value of *CD6* and *CCR7* as diagnostic biomarkers.

Availability of Data and Materials

All the data used in this study are available in GEO (<https://www.ncbi.nlm.nih.gov/geo>) which are public functional genomics data repositories.

Author Contributions

DDX and ZSW designed the research study. DDX and XQL draw the images. DDX and XQL analyzed the data. DDX write the article. All authors contributed to editorial changes in the manuscript. All authors read and approved

the final manuscript. All authors have participated sufficiently in the work and agreed to be accountable for all aspects of the work.

Ethics Approval and Consent to Participate

Not applicable.

Acknowledgment

Not applicable.

Funding

This work was supported by the Natural Science Foundation of Fujian Province (grant number: 2023J01122595).

Conflict of Interest

The authors declare no conflict of interest.

References

- [1] Overland J, Hall C, Holmes A, Burge J. Risk of Intracranial Extension of Craniofacial Dermoid Cysts. *Plastic and Reconstructive Surgery*. 2020; 145: 779e–787e.
- [2] Macdonald RL, Schweizer TA. Spontaneous subarachnoid haemorrhage. *Lancet*. 2017; 389: 655–666.
- [3] Marani W, Mannarà F, Noda K, Kondo T, Ota N, Perrini P, *et al.* Management of an Uncommon Complication: Anterior Choroidal Artery Occlusion by Posterior Clinoid Process Detected Through Intraoperative Monitoring After Clipping of Paraclinoid Aneurysm: 2-Dimensional Operative Video. *Operative Neurosurgery*. 2021; 21: E124–E125.
- [4] Lawton MT, Abla AA, Rutledge WC, Benet A, Zador Z, Rayz VL, *et al.* Bypass Surgery for the Treatment of Dolichoectatic Basilar Trunk Aneurysms: A Work in Progress. *Neurosurgery*. 2016; 79: 83–99.
- [5] Ali MJ, Bendok BR, Tella MN, Chandler JP, Getch CC, Batjer HH. Arterial reconstruction by direct surgical clipping of a basilar artery dissecting aneurysm after failed vertebral artery occlusion: technical case report and literature review. *Neurosurgery*. 2003; 52: 1475–1481.
- [6] Zheng J, Xu R, Guo Z, Sun X. Alanine Aminotransferase Predicts Outcomes in Elderly Patients with Aneurysmal Subarachnoid Hemorrhage. *Current Neurovascular Research*. 2019; 16: 89–95.
- [7] Bakker MK, van der Spek RAA, van Rheenen W, Morel S, Bourcier R, Hostettler IC, *et al.* Genome-wide association study of intracranial aneurysms identifies 17 risk loci and genetic overlap with clinical risk factors. *Nature Genetics*. 2020; 52: 1303–1313.
- [8] Ogilvy CS, Gomez-Paz S, Kicieliniski KP, Salem MM, Akamatsu Y, Waqas M, *et al.* Cigarette smoking and risk of intracranial aneurysms in middle-aged women. *Journal of Neurology, Neurosurgery, and Psychiatry*. 2020; 91: 985–990.
- [9] Zhang X, Zhang H, Shen B, Sun XF. Chromogranin-A Expression as a Novel Biomarker for Early Diagnosis of Colon Cancer Patients. *International Journal of Molecular Sciences*. 2019; 20: 2919.
- [10] Babu RA, Paul P, Purushottam M, Srinivas D, Somanna S, Jain S. Differential expression levels of collagen 1A2, tissue inhibitor of metalloproteinase 4, and cathepsin B in intracranial aneurysms. *Neurology India*. 2016; 64: 663–670.
- [11] Bacigaluppi S, Piccinelli M, Antiga L, Veneziani A, Passerini T, Rampini P, *et al.* Factors affecting formation and rupture of in-

- tracranial saccular aneurysms. *Neurosurgical Review*. 2014; 37: 1–14.
- [12] Zhang J, Shen H, Wang M, Nie S, Wu X, Huang Y, *et al*. Significant Association of CXCL12 rs1746048 with LDL-C Level in Intracranial Aneurysms. *Current Neurovascular Research*. 2018; 15: 26–33.
- [13] Wang J, Wei L, Lu H, Zhu Y. Roles of inflammation in the natural history of intracranial saccular aneurysms. *Journal of the Neurological Sciences*. 2021; 424: 117294.
- [14] Pan JW, He LN, Xiao F, Shen J, Zhan RY. Plasma gelsolin levels and outcomes after aneurysmal subarachnoid hemorrhage. *Critical Care*. 2013; 17: R149.
- [15] Rodemerk J, Junker A, Chen B, Pierscianek D, Dammann P, Darkwah Oppong M, *et al*. Pathophysiology of Intracranial Aneurysms: COX-2 Expression, Iron Deposition in Aneurysm Wall, and Correlation With Magnetic Resonance Imaging. *Stroke*. 2020; 51: 2505–2513.
- [16] Chalouhi N, Points L, Pierce GL, Ballas Z, Jabbour P, Hasan D. Localized increase of chemokines in the lumen of human cerebral aneurysms. *Stroke*. 2013; 44: 2594–2597.
- [17] Zhang HF, Zhao MG, Liang GB, Song ZQ, Li ZQ. Expression of pro-inflammatory cytokines and the risk of intracranial aneurysm. *Inflammation*. 2013; 36: 1195–1200.
- [18] Denorme F, Rustad JL, Campbell RA. Brothers in arms: platelets and neutrophils in ischemic stroke. *Current Opinion in Hematology*. 2021; 28: 301–307.
- [19] Lei TY, Ye YZ, Zhu XQ, Smerin D, Gu LJ, Xiong XX, *et al*. The immune response of T cells and therapeutic targets related to regulating the levels of T helper cells after ischaemic stroke. *Journal of Neuroinflammation*. 2021; 18: 25.
- [20] Quan K, Wang A, Zhang X, Meng X, Chen P, Li H, *et al*. Neutrophil to lymphocyte ratio and adverse clinical outcomes in patients with ischemic stroke. *Annals of Translational Medicine*. 2021; 9: 1047.
- [21] Chatzizisis YS, Baker AB, Sukhova GK, Koskinas KC, Papafaklis MI, Beigel R, *et al*. Augmented expression and activity of extracellular matrix-degrading enzymes in regions of low endothelial shear stress colocalize with coronary atheromata with thin fibrous caps in pigs. *Circulation*. 2011; 123: 621–630.
- [22] Wenjing F, Tingting T, Qian Z, Hengquan W, Simin Z, Agyare OK, *et al*. The role of IL-1 β in aortic aneurysm. *Clinica Chimica Acta*; *International Journal of Clinical Chemistry*. 2020; 504: 7–14.
- [23] Cheng WT, Wang N. Correlation between MMP-2 and NF- κ B expression of intracranial aneurysm. *Asian Pacific Journal of Tropical Medicine*. 2013; 6: 570–573.
- [24] Gangemi RM, Swack JA, Gaviria DM, Romain PL. Anti-T12, an anti-CD6 monoclonal antibody, can activate human T lymphocytes. *Journal of Immunology*. 1989; 143: 2439–2447.
- [25] Bughani U, Saha A, Kuriakose A, Nair R, Sadashivarao RB, Venkataraman R, *et al*. T cell activation and differentiation is modulated by a CD6 domain 1 antibody Itolizumab. *PLoS ONE*. 2017; 12: e0180088.
- [26] Hernández P, Moreno E, Aira LE, Rodríguez PC. Therapeutic Targeting of CD6 in Autoimmune Diseases: A Review of Cuban Clinical Studies with the Antibodies IOR-T1 and Itolizumab. *Current Drug Targets*. 2016; 17: 666–677.
- [27] Chalmers SA, Ayilam Ramachandran R, Garcia SJ, Der E, Herlitz L, Ampudia J, *et al*. The CD6/ALCAM pathway promotes lupus nephritis via T cell-mediated responses. *The Journal of Clinical Investigation*. 2022; 132: e147334.
- [28] Sánchez-Sánchez N, Riol-Blanco L, de la Rosa G, Puig-Kröger A, García-Bordas J, Martín D, *et al*. Chemokine receptor CCR7 induces intracellular signaling that inhibits apoptosis of mature dendritic cells. *Blood*. 2004; 104: 619–625.
- [29] Yanagawa Y, Onoé K. CCR7 ligands induce rapid endocytosis in mature dendritic cells with concomitant up-regulation of Cdc42 and Rac activities. *Blood*. 2003; 101: 4923–4929.
- [30] Halvorsen B, Dahl TB, Smedbakken LM, Singh A, Michelsen AE, Skjelland M, *et al*. Increased levels of CCR7 ligands in carotid atherosclerosis: different effects in macrophages and smooth muscle cells. *Cardiovascular Research*. 2014; 102: 148–156.
- [31] Gaieb Z, Lo DD, Morikis D. Molecular Mechanism of Biased Ligand Conformational Changes in CC Chemokine Receptor 7. *Journal of Chemical Information and Modeling*. 2016; 56: 1808–1822.
- [32] Hauser MA, Kindinger I, Laufer JM, Späte AK, Bucher D, Vanes SL, *et al*. Distinct CCR7 glycosylation pattern shapes receptor signaling and endocytosis to modulate chemotactic responses. *Journal of Leukocyte Biology*. 2016; 99: 993–1007.
- [33] Llodrá J, Angeli V, Liu J, Trogan E, Fisher EA, Randolph GJ. Emigration of monocyte-derived cells from atherosclerotic lesions characterizes regressive, but not progressive, plaques. *Proceedings of the National Academy of Sciences of the United States of America*. 2004; 101: 11779–11784.
- [34] Aoki T, Nishimura M. Targeting chronic inflammation in cerebral aneurysms: focusing on NF-kappaB as a putative target of medical therapy. *Expert Opinion on Therapeutic Targets*. 2010; 14: 265–273.
- [35] Kataoka H. Molecular mechanisms of the formation and progression of intracranial aneurysms. *Neurologia Medico-chirurgica*. 2015; 55: 214–229.